PROSPECT FOR THE HIGGS SEARCHES WITH THE ATLAS DETECTOR*

Elzbieta Richter-Was†

on behalf of the ATLAS Collaboration

Institute of Physics, Jagellonian University
Reymonta 4, 30-059 Kraków, Poland
and
Institute of Nuclear Physics, Polish Academy of Sciences
Radzikowskiego 152, 31-342 Kraków, Poland

(Received April 27, 2009)

The investigation of the electroweak symmetry breaking is one of the primary tasks of the experiments at the CERN Large Hadron Collider (LHC). The potential of the ATLAS experiment for the discovery of the Higgs boson(s) in Standard Model and Minimal Supersymmetric Standard Model is presented, with emphasis on studies which have been completed recently.

PACS numbers: 12.15.–y, 12.60.Fr, 14.80.Bn, 14.80.Cp

1. Introduction

The Large Hadron Collider at CERN will play an important role in the investigation of fundamental questions of particle physics. While the Standard Model of electroweak [1] and strong [2] interactions is in excellent agreement with the numerous experimental measurements, the dynamics responsible for the electroweak symmetry breaking are still unknown. Within the Standard Model, the Higgs mechanism [3] is invoked to break the electroweak symmetry. A doublet of complex of scalar fields is introduced, of which a single neutral scalar particle, the Higgs boson, remains after symmetry breaking. Many extensions of this minimal version of the Higgs sector have been proposed. Mostly discussed scenario is the one with two complex Higgs doublets, as realised in the Minimal Supersymmetric Standard

* Presented at the Cracow Epiphany Conference on Hadron Interactions at the Dawn of the LHC, Cracow, Poland, January 5–7, 2009.

† Supported in part by the RTN European Programme MRTN-CT-2006-035505 (HEP-TOOLS, Tools and Precision Calculations for Physics Discoveries at Colliders) and by Polish Ministry of Science and Higher Education — 153/6PR UE/2007/7.

Model (MSSM) [4], resulting in five observable Higgs bosons, three electrically neutral (h, H, A) and two charged $(H^{\pm})$. At tree level their properties like masses, widths and branching fractions can be predicted in terms of only two parameters, typically chosen to be the mass of the CP-odd Higgs boson, m_A, and the tangent of the ratio of the vacuum expectation values of the two Higgs doublets, $\tan\beta$.

Within the Standard Model, the Higgs boson is the only particle which has not been discovered so far. On the basis of theoretical knowledge, the Higgs sector in the Standard Model remains largely unconstrained. While there is no direct prediction for the mass of the Higgs boson, an upper limit of ~ 1 TeV can be inferred from unitarity arguments [5]. Further constraints can be derived under the assumption that the Standard Model is valid only up to a cutoff energy scale Λ, beyond which new physics becomes relevant. The requirement that the electroweak vacuum is stable and that the Standard Model remains perturbative allows to set upper and lower bounds on the Higgs boson mass [5]. For the cutoff scale Λ of the order of the Planck mass $(\tilde{1}.22 \times 10^{19}$ GeV), the Higgs boson mass is required to be in the range $130 < m_H < 180$ GeV. If the new physics appears at the lower mass scales, the bound becomes weaker, *e.g.* for $\Lambda = 1$ TeV the Higgs boson mass is constrained to be $50 < m_H < 800$ GeV.

The direct search at the e^+e^- collider LEP has led to lower bound on its mass of 114.4 GeV at 95% C.L. [6]. Indirectly, high precision electroweak data constrain the mass of the Higgs boson via their sensitivity to loop corrections. Assuming the overall validity of the Standard Model, a global fit [7] to all electroweak data leads to the 95% C.L. limit $m_H < 154$ GeV. The 95% C.L. lower limit obtained from LEP is not used in the determination of this limit. Including it, the limit increases to 185 GeV. With the recently announced preliminary results from direct searches at Tevatron, with 2.0–3.6 fb^{-1} of data analysed at CDF, and 0.9–4.2 fb^{-1} at DØ, the 95% C.L. upper limits on the Higgs boson production are a factor of 2.5 (0.86) times the SM cross-section for a Higgs boson mass of $m_H = 115$ (165) GeV. The mass range excluded at 95% C.L. of a Standard Model Higgs boson has been extended to $160 < m_H < 170$ GeV [8].

The direct search at the e^+e^- collider LEP has led also to limits in the case of the MSSM Higgs bosons [6]. Values of $\tan\beta$ close to one and low m_A ranges are excluded, see Ref. [9]. The Tevatron experiments are reaching sensitivity [10] to search for the charged Higgs boson in decay of $t\bar{t}$ pair with subsequent decay $H^{\pm} \to \tau\nu$ or direct production of $H^{\pm}$ and decay to tb. The reach of searches at the Tevatron [11] for neutral Higgs decaying into τ-pair pair, interpreted in the MSSM context, extends the 95% exclusion region below $\tan\beta = 40$ for $m_A = 120 \div 160$ GeV.

In the following, I will discuss the potential for Higgs boson searches at the Large Hadron Collider with the ATLAS experiment, focusing on prospects for the initial period, *i.e.* $10 \div 30$ fb^{-1} of integrated luminosity at 14 TeV centre-of-mass collision, and on analyses which have been recently revisited and published in Ref. [12].

This new publication contains significant improvements in experimental methods and better understood features of reconstruction algorithms than the previous work [13]. They are partially based on test beam measurements of various detector components or rely on extensive Monte Carlo simulations of the detailed detector response with as built detector geometry [14]. Here I will show final results of the analyses while I would like to address the reader to Ref. [14] and Ref. [12] for the discussion of the expected detector performance for triggering given topologies or reconstructing physics objects (electrons, photons, muons, taus).

2. Standard Model Higgs bosons at hadron colliders

At hadron colliders the Higgs bosons can be produced via four different processes:

- gluon fusion, $gg \to H$, which is mediated at the lowest order by a heavy top-quark loop;
- vector boson fusion (VBF), $qq \to qqH$;
- associated production of the Higgs boson with weak gauge bosons, $qq \to W/ZH$;
- associated Higgs boson production with heavy quarks, $gg, q\bar{q} \to t\bar{t}H$, $gg, q\bar{q} \to b\bar{b}H$ (and $gb \to bH$).

For all production processes higher-order QCD corrections have been calculated; in particular, significant progress has been made over the last few years in calculation of QCD corrections for gluon-fusion and for the associated $t\bar{t}H$ and $b\bar{b}H$ production processes, for a recent review see [15]. The production cross-section for the different processes is shown in Fig. 1 (left), following recent estimates [12] with NLO accuracy whenever available. Due to impressive progress in the calculation of the higher-order QCD corrections for signal and backgrounds over the past few years, the LHC physics studies have started to use these calculations.

The branching fractions of the Standard Model Higgs boson are shown in Fig. 1 (right), as a function of the Higgs boson mass. When kinematically accessible, decays of the Standard Model Higgs boson into vector boson pairs WW or ZZ dominate over other decay modes. Above the kinematical threshold, the branching fraction to $t\bar{t}$ can reach 20%. All other fermionic decay modes are only relevant for the Higgs boson masses below $2m_W$, with $H \to b\bar{b}$ dominating below 140 GeV. The branching fraction for $H \to \tau\tau$ reaches up to about 8% at the Higgs boson masses between 100–120 GeV. Decays into photon pairs, which are of interest due to their relatively clean signature, can reach branching fraction of up to 2×10^{-3} at low Higgs boson masses.

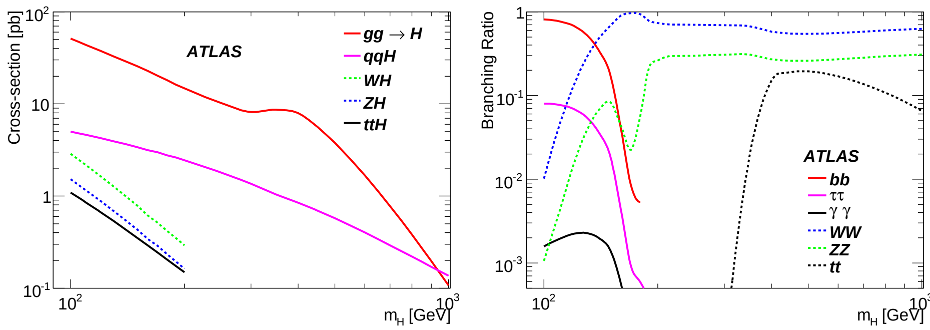

Fig. 1. Right: cross-sections for the five production channels of the Standard Model Higgs boson at the LHC at 14 TeV. Left: branching ratio for the relevant decay modes of the Standard Model Higgs boson as a function of its mass. From Ref. [12].

3. Prospects in the Standard Model Higgs boson searches

The Standard Model Higgs boson will be searched for at the LHC in various decay channels. Over the past ten years, strategies for signal observability and background rejection methods have been established in many studies [13].

In the following I will discuss four of the most important decay channels, for which studies have been recently revisited with the ATLAS experiment and which are included in the most recent combination results.

3.1. The $H \to \gamma\gamma$ decays

The decay $H \to \gamma\gamma$ is a rare decay mode, which is detectable only in the limited Higgs boson mass region 100–150 GeV. Excellent energy and angular resolution are required to observe the narrow mass peak above the irreducible prompt $\gamma\gamma$ continuum and the reducible background resulting from direct photon production or from two-jet production via QCD jets processes. In the recent evaluation different topologies have been studied, *i.e.* only inclusive analysis requiring photon pair in the final state or in association with one or two high p_{T} jets. In addition to the diphoton invariant mass, other discriminating variables are incorporated into the analysis and combined by means of an unbinned maximum-likelihood fit. Photon reconstruction properties and the event topology are used to separate the sample into categories that are fit simultaneously. The inclusive analysis leads to the highest expected signal but also background rates. The expected cross-sections (in fb) are given in Table I. The relative contribution from events with at least one fake photon constitutes 39% of the total background. The theoretical uncertainties of the predictions for prompt single and double photon production used in the inclusive analysis have been evaluated and are summarised in Table II. Diphoton invariant mass spectrum after the application of cuts of the inclusive analysis is shown in Fig. 2 (left). The hatched histograms present contribution from events with one or two fake photons. Selecting more exclusive topologies like $H + 1j$, $H + 2j$ leads to better signal-to-background ratio but much fewer signal events.

TABLE I

Expected cross-sections (in fb) for different signal ($m_H = 120$ GeV) and background processes within a mass window of $m_{\gamma\gamma}\pm 1.4$ of the mass resolution (1.46 ± 0.01) GeV in the no-pileup case and after selection for inclusive analysis. From Ref. [12].

Signal process	Cross-section (fb)	Background process	Cross-section (fb)
$gg \to H$	21	$\gamma\gamma$	562
$VBFH$	2.7	Reducible γj	318
$t\bar{t}H$	0.35	Reducible jj	49
VH	1.3	$Z \to e^+e^-$	18

TABLE II

Summary of the relative systematic uncertainties on the $\gamma\gamma$ and γj processes. From Ref. [12].

Potential sources	$\gamma\gamma$	γj
Scale dependence	14%	20%
Fragmentation	5%	1%
PDF	6%	7%
Total	16%	21%

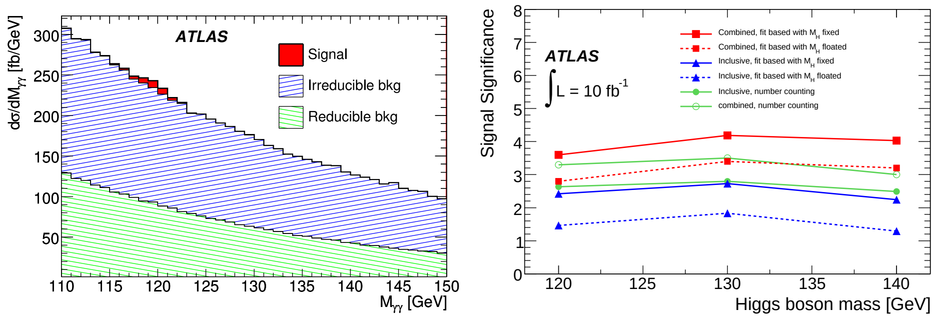

Fig. 2. Left: diphoton invariant mass spectrum after the application of cuts of the inclusive analysis. Right: expected signal significance, as a function of the Higgs mass, for the $H \to \gamma\gamma$ decay assuming an integrated luminosity of 10 fb^{-1}. From Ref. [12].

The expected signal significance for the Higgs boson using the $H \to \gamma\gamma$ decay for 10 fb^{-1} of the integrated luminosity as a function of mass is shown in Fig 2. The sensitivity of the inclusive analysis based on the events counting and the sensitivity when the Higgs boson plus jet is required are shown separately. In addition, shown is also the sensitivity obtained using more elaborate techniques like one dimensional fits with a fixed and floating Higgs boson mass, respectively. A signal significance based on events counting of 2.6 (4.6) can be reached with an integrated luminosity of 10 (30) fb^{-1} for a Higgs mass of 120 GeV in the case of inclusive analysis. The addition of search in association with jets enhances the event counting signal significance to 3.3 (5.7) with 10 (30) fb^{-1}. The sensitivity can be further enhanced by means of unbinned maximum-likelihood fit dividing samples into categories, depending on the event topology and exploiting a number of discriminating variables. An increase up to 3.6 (2.8) at 10 fb^{-1} integrated luminosity in case of fixed (floating) mass fit can be expected.

3.2. *The $H \to ZZ^{(*)} \to 4\ell$ and $H \to ZZ \to 4\ell$ decays*

The decay channel $H \to ZZ^{(*)} \to 4\ell$ provides a rather clean signature in the mass range 120 GeV $< m_H < 2\ m_Z$ and is the most reliable one for the discovery in the range $2\ m_Z < m_H <$ 700 GeV. In addition to the irreducible backgrounds from ZZ^* and $Z\gamma^*$ production, there are large reducible backgrounds from $t\bar{t}$ and $Zb\bar{b}$ production. It has been shown that with expected performance of the detector [14] the reducible background can be suppressed well below the irreducible $ZZ^*/\gamma^* \to 4\ell$, calorimeter and track isolation of leptons together with impact parameter measurements can be used to achieve necessary background rejection against QCD jets and nonisolated leptons from semileptonic decays of heavy flavour quarks. The NLO cross-sections after the full event selection, are shown in Table III. for the three decay channels combined.

TABLE III

Expected cross-sections (in fb) for signal and backgrounds after full selection within the mass window $m_H \pm \sigma_{m_H}$, where σ_{m_H} is the experimental 4-lepton mass resolution, $\sigma_{m_H} = 1.4\% - 1.8\%\ m_H$ for the mass values shown here. The expected significance is given for an integrated luminosity of 30 fb^{-1}. Systematic errors are not yet taken into account in significance calculation. The $t\bar{t}$ background is assumed not to contribute to significance.

Mass	130 GeV	150 GeV	180 GeV
Signal	0.816	1.94	1.32
ZZ^*/γ^*	0.150	0.151	0.938
$Zb\bar{b}$	0.047	0.021	0.013
$t\bar{t}$	< 0.04	< 0.04	< 0.04
Significance (30 fb^{-1})	7.1	14.2	6.2

The reconstructed 4-lepton mass for signal and background processes, in the case of a 130 GeV Higgs boson, normalized to the luminosity of 30 fb^{-1} is shown in Fig. 3 (left). The expected signal significances computed using Poisson statistics, for each of the three decay channels, and their combination are shown in Fig. 3 (right) without including systematic uncertainties. The

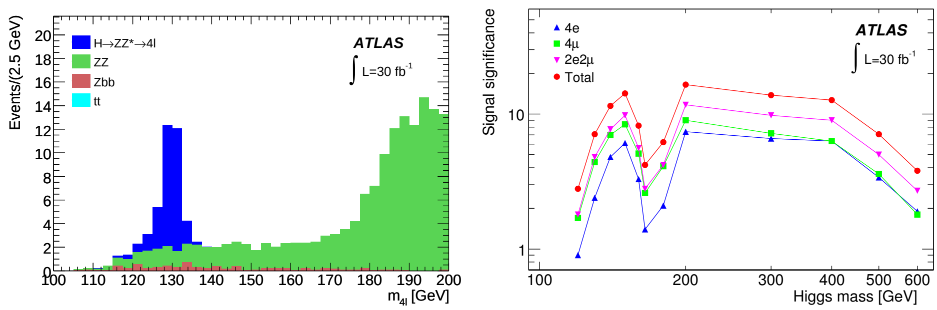

Fig. 3. Reconstructed 4-lepton mass for signal and background processes, in the case of a 130 GeV Higgs boson, normalized to an integrated luminosity of 30 fb^{-1}. Expected signal significances are computed using Poisson statistics, for each of the three decay channels, and their combination (systematic uncertainties not included). From Ref. [12].

significance is slightly reduced if the systematic uncertainties are included; in this case the significance is evaluated using the profile likelihood ratio method [12]. For an integrated luminosity of 30 fb^{-1}, the discovery of the Higgs boson in the 4ℓ channel alone in a mass range 130–500 GeV will be possible, with the exception of the region around 160 GeV of the WW turn on. The $H \to ZZ \to 4\ell$ channel is highly sensitive in the high mass region, 200–400 GeV, and in the 150 GeV region where the Higgs boson should be discovered with an integrated luminosity of 5 fb^{-1}.

3.3. The $qqH \to qq\tau\tau$ decays

A significant discovery potential in the low mass region can be expected when searching for the decay into pair of τ leptons and of Higgs bosons produced in association with two jets (mainly by the Vector Boson Fusion process). The analysis requires excellent performance for every detector subsystem: the presence of the τ decays implies final states with electrons, muons, hadronic τ decays and missing transverse momentum, while the Vector Boson Fusion production process introduces jets that tend to be quite forward in the detector. The sensitivity is estimated based on the combination of the lepton–lepton ($\ell\ell$) and lepton–hadron (ℓh) topology for τ-pair decays; the performance in hadron–hadron (hh) channel has been also addressed in most recent analyses [12].

The signal events are produced with significant transverse momenta, so the τ from the decay are boosted which causes their decay products being almost collinear in the laboratory frame. The $\tau\tau$ invariant mass can be therefore reconstructed in the collinear approximation, *i.e.* assuming that the τ direction is given by their visible decay products (charged lepton or hadrons). The mass resolution is about 10 GeV, leading to approximately 3.5% precision on the mass measurement with 30 fb^{-1} of data. Example fits to a data sample with the signal-plus-background for the lh-channel at $m_H = 120$ GeV with 30 fb^{-1} of data is shown in Fig. 4 (left).

In the recent analysis particular emphasis has been placed on data-driven background estimation strategies and the associated uncertainties in normalisation and shape. Expected signal significance for several masses based on fitting the $m_{\tau\tau}$ spectrum is shown in Fig. 4 (right). The results obtained neglecting the pileup effects indicate that a $\sim 5\sigma$ significance can be achieved for the Higgs boson mass in the range 115–125 GeV after collecting 30 fb^{-1} of data and combining the $\ell\ell$ and ℓh channels. The effects induced by the event pile-up has not been fully addressed yet.

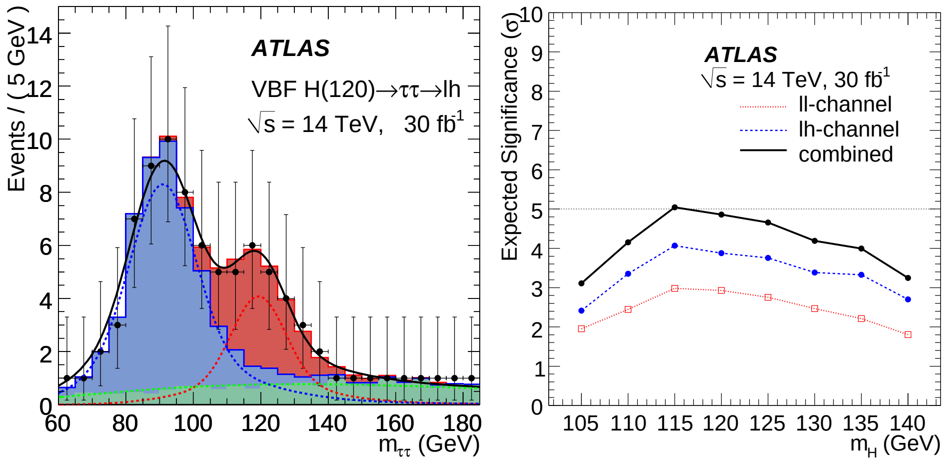

Fig. 4. Example fits to a data sample with the signal-plus-background for the lh-channel at $m_H = 120$ GeV with 30 fb^{-1} of data. Expected signal significance for several masses based on fitting the $m_{\tau\tau}$ spectrum. Background uncertainties are incorporated by utilizing the profile likelihood ratio method. These results do not include the impact of pileup. From Ref. [12].

3.4. *The $gg \to H \to WW$ and $qqH \to qqWW$ decays*

The prospects for the Higgs searches mass range below 200 GeV through the channel $H + 0j$ and the VBF channel $H + 2j$ with $H \to WW \to e\nu\mu\nu$ have been reviewed, with an emphasis on evaluating methods to estimate backgrounds using control samples in data. In the studies of the former one must consider background processes that yield two leptons and significant missing transverse energy in the final state; in the latter, the final state also includes two hard jets (from the struck quarks) which tend to be well-separated in pseudorapidity. In this channel it is not possible to reconstruct the Higgs boson mass peak; instead, an excess of events above the expected backgrounds can be observed and used to establish the presence of the Higgs boson signal, provided the background level can be safely controlled. Usually, the transverse mass computed from the leptons and the missing transverse momentum is used to discriminate between signal and background. In addition, its shape provides additional sensitivity to the true Higgs boson mass.

Signal discrimination from the background relies on a complicated topological selection. The $H + 0j$ analysis requires two opposite-sign isolated leptons, large missing transverse energy, vetoes additional jets and exploits differences from spin correlations effects between signal and backgrounds on the transverse opening angle between leptons.

The lepton selection (identification and isolation) criteria are more stringent than in discussed latter $H+2j$ analysis, since $H+0j$ signature has fewer handles to suppress large reducible backgrounds from $W+$jets and $b\bar{b}$ processes. In Table IV shown is an example of separating signal and background regions with different kinematical selections which can be then used for in-situ normalisation and cross-check on the background predictions.

TABLE IV

Expected cross-sections (in fb) after selection for a cut based analysis with a test mass $m_H = 170$ GeV in the $H+0j, H \to WW \to e\nu\mu\nu$ channel. The $W+$jets and $b\bar{b}$ backgrounds are omitted for this table.

Region	Signal	$t\bar{t}$	WW	$Z \to \tau\tau$
Signal-like	28.65 ± 0.80	1.14 ± 1.14	29.35 ± 1.59	<1.74
Control	1.47 ± 0.27	5.71 ± 2.55	61.13 ± 2.33	4.06 ± 1.53
b-tagged	0	6.85 ± 2.80	0.11 ± 0.09	1.16 ± 0.82

Fig. 5(left) shows the distribution of the transverse opening angle $\Delta\phi^{\ell\ell}$ of the two leptons after preselection cuts for signal and WW background. Fig. 5(right) shows the distribution of the transverse mass $m_{\rm T}$ for events with $\Delta\phi^{\ell\ell} < 1.575$ and $p_{\rm T}^{WW} > 20$ GeV, in a fitted toy Monte Carlo outcome containing the Standard Model Higgs boson with $m_H = 170$ GeV, after 10 fb^{-1} of the integrated luminosity.

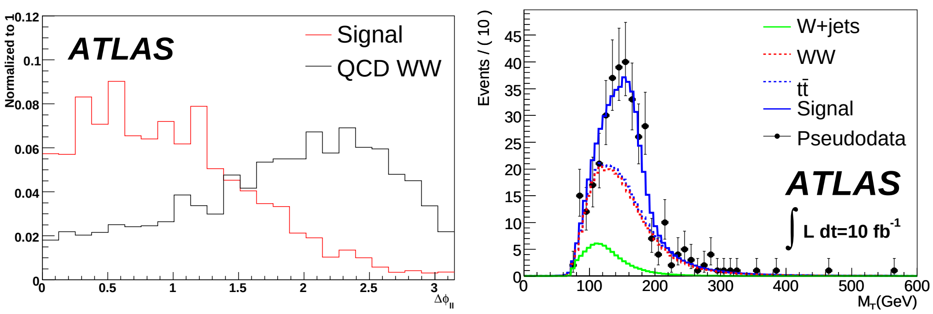

Fig. 5. Left: transverse opening angle $\Delta\phi^{\ell\ell}$ of the two leptons after preselection cuts. Right: transverse mass $m_{\rm T}$ for events with $\Delta\phi^{\ell\ell} < 1.575$ and $p_{\rm T}^{WW} > 20$ GeV (see text). From Ref. [12].

The $H+0j$ channel is very promising for the Higgs boson masses around the WW threshold. An in-situ background normalisation technique has been prepared and it has been shown that the uncertainties can be controlled, and that background can be normalised with a two-dimensional fit in the transverse mass and the $p_{\rm T}$ of the WW system. With 10 fb^{-1} one would expect to be able to reach a 5σ discovery with the $H \rightarrow WW \rightarrow e\nu\mu\nu$ channel alone if there is the Standard Model Higgs boson with a mass between 140 and 180 GeV.

The $H+2j$ analysis explores, in addition, characteristic kinematical features of the accompanying jets (tag jets) from VBF production: pseudorapidity gap between jets, invariant mass of the jet-system and vetoes additional jet activity in the gap region. In Fig. 6 shown are distributions essential for discriminating signal and background events. A requirement of $\eta_1\eta_2 < 0$ and jet $E_{\rm T} > 20$ GeV is used. Distributions are shown for $m_H = 170$ GeV, but the dependence of these variables on the Higgs boson mass is rather weak. This channel has smaller event rate than the $H+0j$ channel but leads to a similar significance.

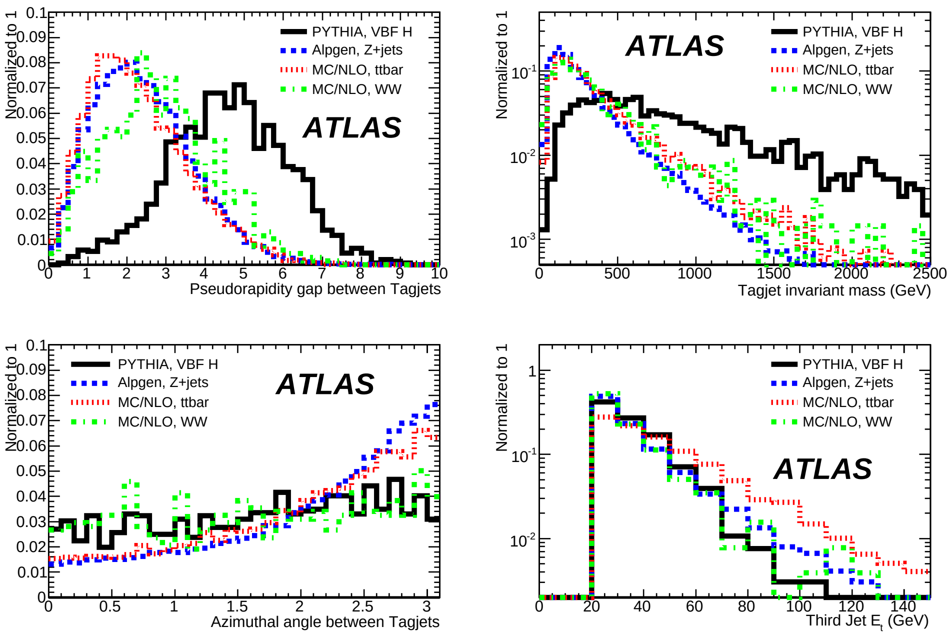

Fig. 6. Pseudorapidity gap between tag jets (left-top), invariant mass distribution of tag jets (right-top), azimuthal angle gap between jets (left-bottom) and transverse energy of the third one (left-right). From Ref. [12].

With 10 fb^{-1} integrated luminosity, one should expect to be able to reach a 5σ discovery in the $H \to WW \to e\nu\mu\nu$ channel alone if there is the Standard Model Higgs boson with a mass between 155 and 180 GeV. Combining the two channels here discussed one would expect to be able to discover the Standard Model Higgs boson in the $H \to WW$ decay mode in the mass range 135–190 GeV. Fig. 7 shows the linearity of the mass determination and the expected significance of a combined fit of the two topologies as a function of a true Higgs boson mass. The grey (green) band represents the width of the gaussian fit to the region around the peak of the best-fit mass distribution and the error bars show the median fit error. With 10 fb^{-1} integrated luminosity one would expect to be able to measure Higgs boson mass with a precision of about 7 GeV for a true mass 130 GeV or about 2 GeV for a true mass 160 GeV.

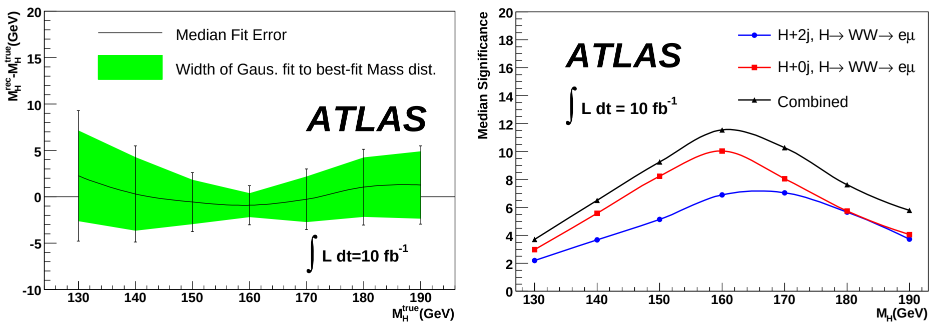

Fig. 7. Left: the linearity of the mass determination for the combined fit of $H{+}0/2j$, $H \to WW \to e\nu\mu\nu$. Right: the expected significance at 10 fb^{-1}. From Ref. [12].

3.5. Statistical combination of Standard Model channels

The Higgs boson searches will exploit a number of statistically independent decay channels. All of the information will be combined to provide a single estimate of the significance of a discovery or exclusion limits on the Higgs production. The approach taken in most recent studies [12] is based on frequentist statistical methods, where effects of systematic uncertainties are incorporated by the use of the profile likelihood ratio. The profile likelihood ratio treats systematic errors by associating the uncertainties with adjustable (nuisance) parameters and adjusting those to maximize the likelihood.

For different hypothesised Standard Model Higgs boson mass, the signal significances expected are presented assuming the Standard Model Higgs production rate, as well as the expected upper limits on the Higgs production cross-section, under the hypothesis of no Higgs signal. The studies have exploited a series of useful approximations that allow one to determine the median discovery and exclusion sensitivities from a combined fit. The validation studies indicate that the approximations used should be reasonably accurate or lead to conservative limits for integrated luminosity over 2 fb^{-1}. For earlier stages of the experiment it is expected that one will need to rely on Monte Carlo methods, which should be feasible for exclusion limits at the 95% confidence level.

The procedure for the combination of search results based on the profile likelihood ratio has been applied to a study of the search for the Standard Model Higgs boson using four search channels: $H \to \tau^+\tau^-$, $H \to W^+W^- \to e\nu\mu\nu$, $H \to \gamma\gamma$ and $H \to ZZ^{(*)} \to 4\ell$. The resulting significances per channel and the combined one are shown in Fig. 8 for 10 fb^{-1} integrated luminosity. The median p-value obtained for excluding the Standard Model Higgs Boson for the various channels, as well as the combination for the lower mass range (left) and for masses up to 600 GeV (right) mass range, are shown in Fig. 9.

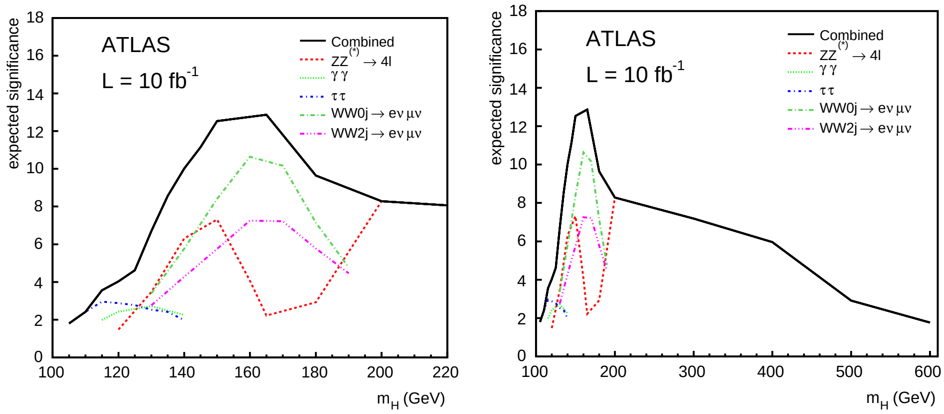

Fig. 8. The median discovery significance for the Standard Model Higgs Boson for the various channels as well as the combination for the integrated luminosity of 10 fb^{-1} for (left) the lower mass range (right) for masses up to 600 GeV. From Ref. [12].

There is a decrease in expected significance for low m_H; however further developments of the analysis will allow to increase the sensitivity in this region: for example improving analysis methods for $H \to \gamma\gamma$ channel with separation of channels into zero or two accompanying jets topology. Additional final states such as ttH and WH/ZH with $H \to b\bar{b}$ will help somewhat, although the contribution to the sensitivity will be small because of the large uncertainties in the background. For the WW channel,

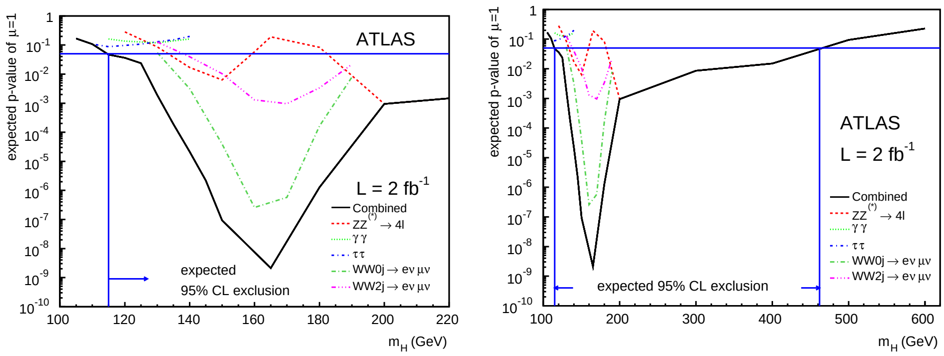

Fig. 9. The median p-value obtained for excluding the Standard Model Higgs Boson for the various channels as well as the combination for (left) the lower mass range (right) for masses up to 600 GeV. From Ref. [12].

the present studies include only $e\nu\mu\nu$ decay mode, but it is planned to explore $e\nu e\nu$, $\mu\nu\mu\nu$ and $qq\ell\nu$ as well. The additional WW and $ZZ^{(*)}$ modes not discussed here, have been shown in past to enhance sensitivity for a high mass Higgs.

The results obtained confirm the good discovery and exclusion sensitivities already shown in ATLAS Technical Design Report [13]. With a luminosity of 2 fb^{-1} the expected (median) sensitivity is at the 5σ level or greater for discovery of the Higgs boson in the mass range 143–179 GeV, and the expected lower limit at 95% confidence level on the Higgs mass is about 115 GeV.

4. Prospects in the MSSM Higgs boson searches

The LHC experiments have a large potential in the investigation of the MSSM Higgs sector. In the MSSM the couplings of Higgs bosons to fermions and bosons are different from those in the Standard Model resulting in different production cross-sections and decay rates. While decays into ZZ and WW are dominant in the Standard Model, for Higgs masses above $m_H \sim 160$ GeV, in the MSSM these decay modes are either suppressed like $\cos(\beta - \alpha)$ in the case of the H (where α is the mixing angle of the two CP-even Higgs bosons) or even absent in the case of A. Instead, the coupling of the Higgs bosons to third generation fermions is strongly enhanced for large regions of the parameter space.

The search for light neutral Higgs bosons is based on the same channels considered for the Standard Model Higgs case. Heavier Higgs bosons will be searched for with the analysis of additional decay channels which become accessible in certain regions of the MSSM parameter space, due to enhanced couplings. Example are the decay modes $H/A \to \tau\tau$ and $H/A \to \mu\mu$, relevant for large values of $\tan\beta$. Decays into τ leptons also contribute to the search for charged Higgs bosons, which at the LHC can be extended to masses beyond the top-quark mass. The comprehensive study of the ATLAS detector discovery potential has been presented in [13]. These studies have provided the first complete results for the ATLAS detector. Since then, they have been updated to include more studies on MSSM models [17]. In the most recent publication [12], more detailed analyses based on as-installed detector simulation as well as more recent Monte Carlo generators have been revisited for the most important channels, with emphasis on the data-driven analysis of the background systematics and elaborate statistical methods for combination, as discussed in the Standard Model case.

Below I recall, as present available, the preliminary picture for different benchmark scenarios, and in more details discuss analyses which have been revisited recently for $H^{\pm} \to \tau\nu$, $H/A \to \tau\tau \to \ell\ell 4\nu$ and $H/A \to \mu\mu$ searches.

4.1. The MSSM discovery potential in various benchmark scenarios

Different benchmark scenarios have been proposed for the interpretation of the MSSM Higgs boson searches [16]. In the MSSM, the masses and couplings of the Higgs bosons depend, in addition to $\tan\beta$ and m_A, on the other parameters through radiative corrections. In particular, the phenomenology of the light Higgs boson h depends on the scenario and the following ones have been considered as representative ones:

- m_h*-max*: the SUSY parameters are chosen in such way that for each point in the $(m_A, \tan\beta)$ parameter space the lightest Higgs boson mass m_h close to the maximum possible value is obtained.
- *No-mixing scenario*: vanishing mixing in the stop sector is assumed, this scenario typically gives a small mass of the lightest Higgs boson h and is less favorable for the LHC.
- *Gluophobic scenario*: the effective coupling of the light Higgs to gluons is strongly suppressed as the consequence of the strong mixing in the stop sector.
- *Small α scenario*: the parameters are chosen in such way that the effective mixing angle between the CP-even Higgs bosons is small. This results in the reduced branching ratio into $b\bar{b}$ and $\tau\tau$ for large $\tan\beta$ and intermediate values of m_A.

The overall discovery potential for the four scenarios is presented in Fig. 10. for the integrated luminosity of 30 fb^{-1}. The full parameter space can be covered for all benchmarks. However, in the region of moderate $\tan\beta$ and large m_A only, one MSSM Higgs boson, the lightest Higgs boson (h) can be discovered. This remains true even for the 300 fb^{-1} integrated luminosity. The exact location of that region depends on details of the considered model.

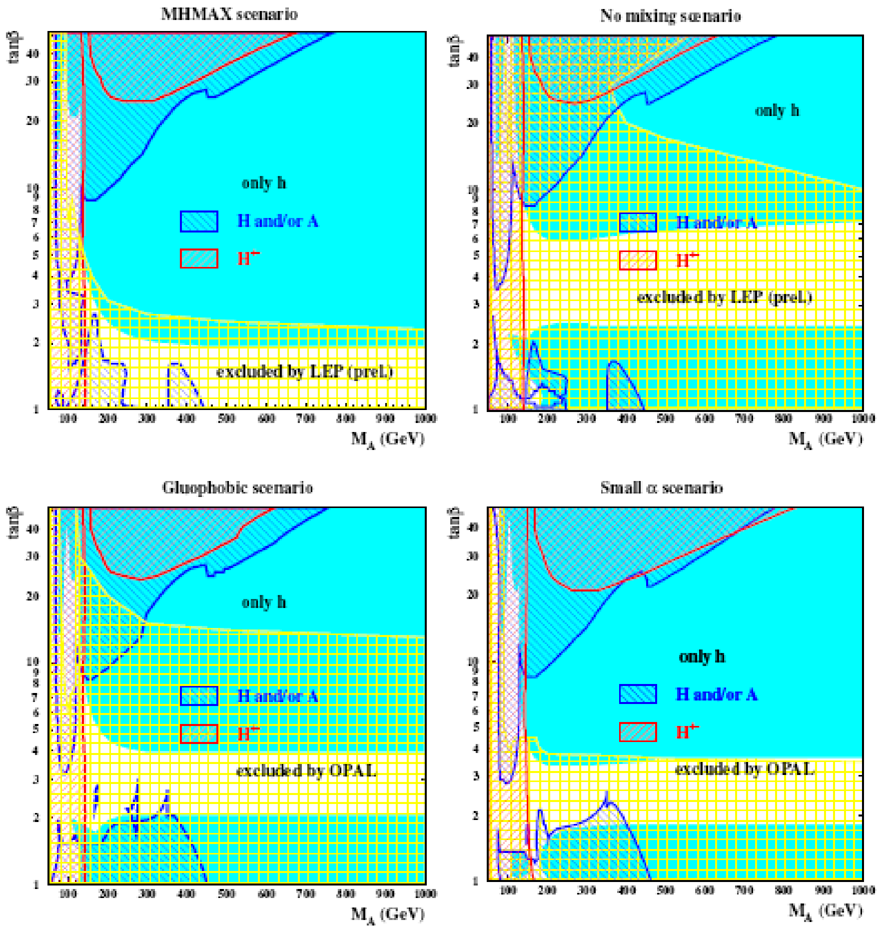

Fig. 10. Discovery potential for the Higgs bosons discovery in different benchmark scenarios (see text). In the grey (blue) area only lightest Higgs boson h can be observed. In the blue hatched area the heavy neutral Higgs bosons H and/or A, and in the red hatched area the charged Higgs bosons $H^{\pm}$ can be detected. The cross-hatched yellow region is excluded by searches at LEP. ATLAS preliminary results [17].

For the above benchmark scenarios it was assumed that CP is conserved in the Higgs sector. Although CP conservation is present at Born level, CP violating effects might be introduced via complex mixing parameters A_t, A_b or mass terms. As a consequence, the mass eigenstates H_1, H_2 and H_3 are mixture of the CP eigenstates: h, H and A. A special scenario considered as a benchmark one is the so called CPX scenario [18], which is characterised by large phases. In this scenario, uncovered by LEP region in parameter space exists for the H_1, the lightest mass eigenstate [19]. Preliminary studies have shown, that even at the LHC, uncovered regions at medium $\tan\beta \sim 5$ and small $m_{H^\pm}$ around 150 GeV which corresponds to small H_1 masses — remain, as illustrated in Fig. 11. It needs to be studied further if can be cover by exploiting additional search channels. A similar situation may occur in the context of the next-to-minimal Standard Model (NMSSM).

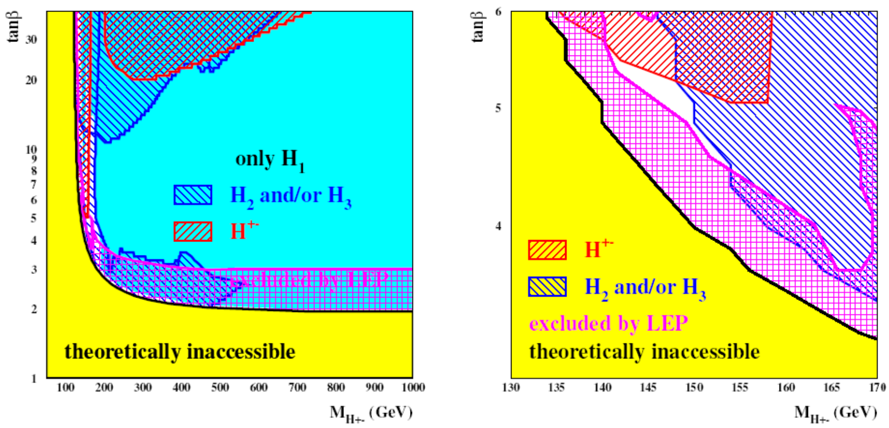

Fig. 11. Overall discovery potential for the Higgs bosons in the CPX scenario for data corresponding to the integrated luminosity of 300 fb^{-1}. The cross-hatched yellow region is excluded by searches at LEP. ATLAS preliminary results [19].

4.2. Charged Higgs bosons

The discovery of the charged Higgs boson would be a tangible proof of physics beyond the Standard Model. The recent studies present potential for discovery in search for five different final states arising from the three dominating fermionic decay modes. The prepared search analyses cover the region below the top-quark mass, taking into account present experimental constraints, the transition region with the charged Higgs boson mass of the order of top-quark mass, and the high mass region with the charged Higgs boson mass up to 600 GeV.

The sensitivities for discovery and exclusion are calculated with the profile likelihood method, combining all channels and including systematic and statistical uncertainties. The results are summarised in combined discovery and exclusion contours shown in Fig. 12 for m_h-max scenario. The dependence of the $H^{\pm}$ discovery sensitivity on the specific choice of the MSSM parameter values is rather small, with the exception of the Higgsino mixing parameter. A significant improvement of present days constraints can already be achieved with limited but well understood data (less than 1 fb^{-1}).

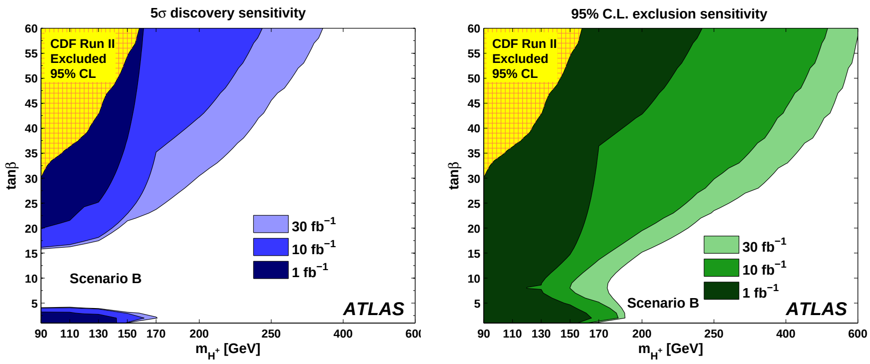

Fig. 12. Scenario B (m_h-max): Combined results. Left: Discovery contour, Right: Exclusion contour. Systematic and statistical uncertainties are included. From Ref. [12].

Below the top-quark mass the charged Higgs bosons are predominantly produced in top-quark decays and the main decay mode is $H^+ \to \tau\nu$. Three different combinations of final states have been studied separately (τ and W bosons decaying leptonically and/or hadronically) each of them has shown to have potential for overperforming present sensitivity of Tevatron experiments already with 1 fb^{-1}. Analyses for adding also di-lepton final states are underway. However, for the intermediate $\tan\beta \sim 7$, no discovery sensitivity is present, although the production of this boson can be excluded in this region. This reduced sensitivity (*vs* previous estimates) represents rather conservative approach taken due to insufficient statistics available in MC samples to estimate systematic uncertaintities, the sensitivity is recovered in the no-systematics limit.

The search for the heavy charged Higgs boson ($m_{H^{\pm}} > m_t$) at Tevatron has been recently reported in [20], see also review article [21]. At the LHC, the main production mode will be the gb fusion ($gb \to tH^+$). According to current expectations the discovery potential will be primarily in $\tau\nu$ decay channel even if the dominant mode is decay to tb quarks. The discovery reached in $\tan\beta$ strongly depends on the Higgs boson mass.

In general, the ATLAS experiment will have sensitivity to explore the charged Higgs sector over sizable region of the parameter space with first 10 fb^{-1}. For a high SUSY mass scale, the charged Higgs boson could be the first signal of New Physics (and indication for Supersymmetry) discovered.

4.3. The heavy Higgs bosons in $H/A \to \tau^+\tau^-$ channel

The coupling of the Higgs bosons to third generation fermions is strongly enhanced for large regions of the parameter space. The decay of the neutral Higgs bosons into pair of τ leptons therefore constitutes an important discovery channel at LHC. The production of the Higgs bosons can proceed via two different processes; gluon-fusion or production in association with b-quarks. The highest sensitivity is expected [13] in the lepton–hadron final state of tau decays, and statistical combination of topologies with 0 b-jet (dominating medium $\tan\beta$) and one b-jet (dominating at higher $\tan\beta$ regions).

Recently, [12], detailed analysis for the $h/H/A \to \tau^+\tau^- \to \ell^+\ell^- 4\nu$ final state, with at least 1 b-jet identified as coming from b-quark, has been performed. Particular emphasis was put on the data-driven procedure to estimate shape and normalisation of the resonant $Z \to \tau\tau$ background, dominant in low mass region, from measurements of the $Z \to ee$ and $Z \to \mu\mu$ channels with the data. The expected discovery potential and exclusion limits are shown in Fig. 13 for 30 fb^{-1}.

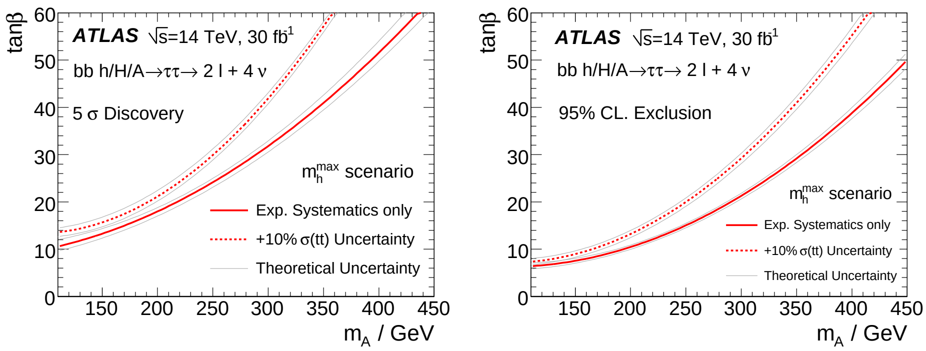

Fig. 13. The five σ discovery potential (left) and the 95% exclusion limit (right) as a function of m_A and $\tan\beta$. The solid line represents the main result of the analysis. The dashed lines indicate the discovery potential and exclusion limit including an addition 10% uncertainty on the tt cross-section. The bands represent the influence of the systematic uncertainty on the signal cross-section. From Ref. [12].

Although the discovery potential of the lepton–lepton channel is weaker than in the lepton–hadron channel, such measurement may be easier at the beginning as does not require identification of the hadronically decaying τ leptons.

4.4. The heavy Higgs bosons in $H/A \to \mu^+\mu^-$ channel

The decay of neutral MSSM Higgs bosons A, H and h into two muons is strongly enhanced in the MSSM for large values of $\tan\beta$ (for the h if far from the decoupling limit), and can be explored either as a discovery channel or for the exclusion of a large region of the $m_A - \tan\beta$ parameter space. Although the $\mu^+\mu^-$ signature has substantially smaller branching ratio if compared to $\tau\tau$ channel (scales as $(m_\mu/m_\tau)^2$) it has the advantage of very clean signature in the detector, which allows also for a precise and direct Higgs boson mass measurement. The event selection criteria are optimised in the signal mass range from 100 to 500 GeV, separately for the signature with 0 b-jets (for the direct production in gluon fusion) and with at least 1 b-jet in the final state (for associated production with b-quarks, strongly enhanced at large $\tan\beta$).

The obtained combined results, presented in Fig. 14 show that the integrated luminosity of 10 fb^{-1} will allow for the discovery for m_A masses up to 350 GeV with $\tan\beta$ values between 30–60. The three times higher luminosity allows to increase sensitivity down to $\tan\beta = 20$. The theoretical and detector-related systematic uncertainties are estimated to degrade the signal significance by up to 20%. Given the good mass resolution for di-muon final states, this channel can eventually be used to separate nearby Higgs boson resonances using a precise measurement of the shape of mass distributions.

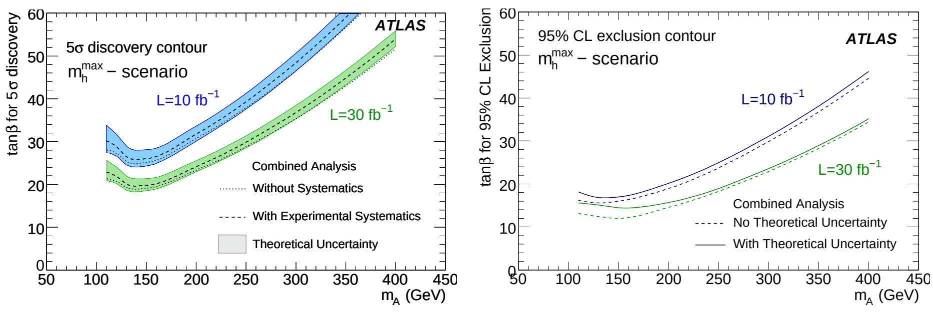

Fig. 14. Combined analyses results: (left) $\tan\beta$ values needed for the 5σ-discovery at 10 fb^{-1} and 30 fb^{-1} of the integrated luminosity, shown is dependence on the A boson mass and (right) combined 95% C.L. exlucion limits. From Ref. [12].

5. Summary

The ATLAS experiment at LHC is well set up to explore the existence of the Standard Model or the MSSM Higgs bosons and are also prepared for unexpected scenarios.

I have discussed several important channels for the Higgs boson searches, for which analyses have been recently revisited as an important milestone of preparing physics programme for the ATLAS experiment with first 10–30 fb^{-1} of the integrated luminosity.

With respect to previous estimates, analyses have been completed with very detailed studies on the theoretical and detector related systematics, also the data-driven methods for controlling background shapes and normalisation have been established in most cases. The most recent Monte Carlo generators and NLO cross sections have been used for signal and backgrounds if available. In addition, the very advanced statistical procedures to estimate discovery and exclusion reach have been prepared and their performance evaluated on the basis of Monte Carlo studies.

In general, recent studies reported confirm good discovery sensitivities of ATLAS detector for the Standard Model and the MSSM Higgs boson searches. The full Standard Model mass range and the full MSSM parameter space can be covered (for the CP conserving case).

The LHC data will hopefully give soon guidance to the theory and to the future high energy physics experiments.

REFERENCES

[1] S.L. Glashow, *Nucl. Phys.* **22**, 579 (1961); S. Weinberg, *Phys. Rev. Lett.* **19**, 1264 (1967); A. Salam, in *Elementary Particle Theory*, ed. N. Svartholm, Almquist and Wiksell, Stockholm 1968, p. 367.

[2] H.D. Politzer, *Phys. Rev. Lett.* **30**, 1346 (1973); D.J. Gross, F.E. Wilczek, *Phys. Rev. Lett.* **30**, 1343 (1973); H. Fritzsch, M. Gell-Mann, H. Leutwyler, *Phys. Lett.* **B47**, 365 (1973).

[3] P.W. Higgs, *Phys. Rev. Lett.* **12**, 132 (1964); *Phys. Rev.* **145**, 1156 (1966); F. Englert, R. Brout, *Phys. Rev. Lett.* **13**, 321 (1964); G.S. Guralnik, C.R. Hagen, T.W. Kibble, *Phys. Rev. Lett.* **13**, 585 (1964).

[4] For a review see for example: J.F. Gunion, H.E. Haber, G. Kane, S. Dawson, *The Higgs Hunter's Guide, Frontiers in Physics Series*, Vol. 80, Addison-Wesley publ., ISBN 0-201-50935-0; H.P. Nilles, *Phys. Rep.* **110**, 1 (1984); H.E. Haber, G.L. Kane, *Phys. Rep.* **117**, 75 (1985).

[5] L. Maiani, G. Parisi, R. Petronzio, *Nucl. Phys.* **B136**, 115 (1979); N. Cabbibo *et al.*, *Nucl. Phys.* **B158**, 295 (1979); G. Altarelli, G. Isidori, *Phys. Rev. Lett.* **B337**, 141 (1994); J.A. Casas, J.R. Espinosa, M. Quiros, *Phys. Lett.* **B342**, 171 (1995); *Phys. Lett.* **B383**, 374 (1996).

[6] ALEPH, DELPHI, L3 and OPAL Collaborations, *Phys. Lett.* **B565**, 61 (2003).

[7] LEP Electroweak Working Group, July 2008, `http://lepewg.web.cern.ch/LEPEWWG`.

[8] The TEVNPH Working Group (for the CDF and DØ Collaboration), FERMILAB-PUB-09-060-E, CDF Note 9713, DØ Note 5889.

[9] J. Abdallah *et al.* [DELPHI Collaboration], *Eur. Phys. J.* **C54**, 1 (2008), Erratum *Eur. Phys. J.* **C56**, 165 (2008).

[10] A. Abulencia *et al.* [CDF Collaboration], *Phys. Rev. Lett.* **96**, 042003 (2006); V. Abazov *et al.* [DØ Collaboration], `arXiv.org:0807.0859 [hep-ex]`.

[11] A. Abulencia *et al.* [CDF Collaboration], *Phys. Rev. Lett.* **96**, 011802 (2006); V. Abazov *et al.*, [DØ Collaboration], *Phys. Rev. Lett.* **102**, 051804 (2009).

[12] G. Aad *et al.* [ATLAS Collaboration], CERN-OPEN-2008-020, Geneva, 2008, `[arXiv:0901.0512]`.

[13] The ATLAS Collaboration, CERN/LHCC/99-15, 1999.

[14] G. Aad *et al.* [ATLAS Collaboration], Published in *JINST* **3**, S08003 (2008).

[15] K. Jakobs, *Eur. Phys. J.* **C**, `doi:10.1140/epjc/s10052-008-0746-8`.

[16] M. Carena, S. Heinemeyer, C.E. Wagner, G. Weiglein, *Eur. Phys. J.* **C26**, 601 (2003).

[17] M. Schumacher, `hep-ph/0410112`, presented at SUSY04 Conference, October 8th 2004.

[18] M. Carena *et al.*, *Phys. Lett.* **B495**, 155 (2000).

[19] E. Accomando *et al.* CERN-2006-009, Jul 2006, 542pp `[hep-ph/0608079]`.

[20] V. Abazov *et al.* [DØ Collaboration], `arXiv:0807.0859v1 [hep-ex]`.

[21] J.L. Feng, J.-F. Grivaz, J. Nachtman, `arXiv:0903.0046v1 [hep-ex]`.